

The formation of three-grain junctions during
solidification. Part II: theory.
Electronic supplementary material

A. C. Fowler^{1,2} and Marian B. Holness³

¹MACSI, University of Limerick, Limerick, Ireland

²OCIAM, University of Oxford, Oxford, UK

³Department of Earth Science, University of Cambridge, Cambridge,
U. K.

Tuesday 12th April, 2022, 20:24

ESM.1 Derivation of (2.10) from (2.9)

We need to calculate $\phi(\theta)$, where

$$\tan \phi = -\frac{dx}{dy}, \quad (\text{ESM1.1})$$

$x = R(\theta) \cos \theta$ and $y = R(\theta) \sin \theta$ are Cartesian coordinates, and the curve (in polar coordinates) $r = R(\theta)$ is given by

$$\frac{(1 + \gamma)r_0}{\gamma R} = 1 + \frac{1}{\gamma} \cos(\theta - \alpha). \quad (\text{ESM1.2})$$

It follows from (ESM1.1) that

$$\begin{aligned} \tan \phi &= -\frac{\frac{d}{d\theta}[R(\theta) \cos \theta]}{\frac{d}{d\theta}[R(\theta) \sin \theta]} = \frac{R \sin \theta - R' \cos \theta}{R \cos \theta + R' \sin \theta} \\ &= \frac{\frac{1}{R} \sin \theta + \left(\frac{1}{R}\right)' \cos \theta}{\frac{1}{R} \cos \theta - \left(\frac{1}{R}\right)' \sin \theta}. \end{aligned} \quad (\text{ESM1.3})$$

From (ESM1.2), we have

$$\begin{aligned} (1 + \gamma)r_0 \left(\frac{1}{R} \right) &= \gamma + \cos(\theta - \alpha), \\ (1 + \gamma)r_0 \left(\frac{1}{R} \right)' &= -\sin(\theta - \alpha), \end{aligned} \tag{ESM1.4}$$

and therefore from (ESM1.3),

$$\begin{aligned} \tan \phi &= \frac{[\gamma + \cos(\theta - \alpha)] \sin \theta - \sin(\theta - \alpha) \cos \theta}{[\gamma + \cos(\theta - \alpha)] \cos \theta + \sin(\theta - \alpha) \sin \theta} \\ &= \frac{\gamma \sin \theta + \sin \alpha}{\gamma \cos \theta + \cos \alpha}, \end{aligned} \tag{ESM1.5}$$

which is (2.10).

ESM.2 The geometry of conics

In section 3 of the paper, much use is made of the geometry of conics, as deduced from their polar coordinate representation. In this section we elucidate this material. We start with equation (3.3) which we may write in the form

$$\frac{d}{r} = \gamma - \cos \theta, \tag{ESM2.1}$$

where $\gamma = \frac{1}{e} < 1$. Converting this to Cartesian coordinates gives $d + x = \gamma \sqrt{x^2 + y^2}$, and squaring this leads to

$$(1 - \gamma^2) \left[x + \frac{d}{1 - \gamma^2} \right]^2 - \gamma^2 y^2 = \frac{d^2 \gamma^2}{1 - \gamma^2}, \tag{ESM2.2}$$

which, after an origin shift to $X = x + \frac{d}{1 - \gamma^2}$, can be converted to the standard form

$$\frac{X^2}{a^2} - \frac{y^2}{b^2} = 1, \tag{ESM2.3}$$

where

$$a = \frac{d\gamma}{1 - \gamma^2}, \quad b = \frac{d}{(1 - \gamma^2)^{1/2}}. \tag{ESM2.4}$$

This gives the standard form of the hyperbola shown in figure ESM.1. It should be noted that the squaring of $d + x = \gamma r$ gives two branches of (ESM2.3), but the polar representation (ESM2.1) only has one.

It is clear from (ESM2.1) that the asymptotic rays of the hyperbola are $\theta = \pm \alpha = \pm \cos^{-1} \gamma$, and this provides an easy way to visualise the hyperbola, from the graph of r (or $\frac{1}{r}$) against θ . Care needs to be taken, because one might be tempted to

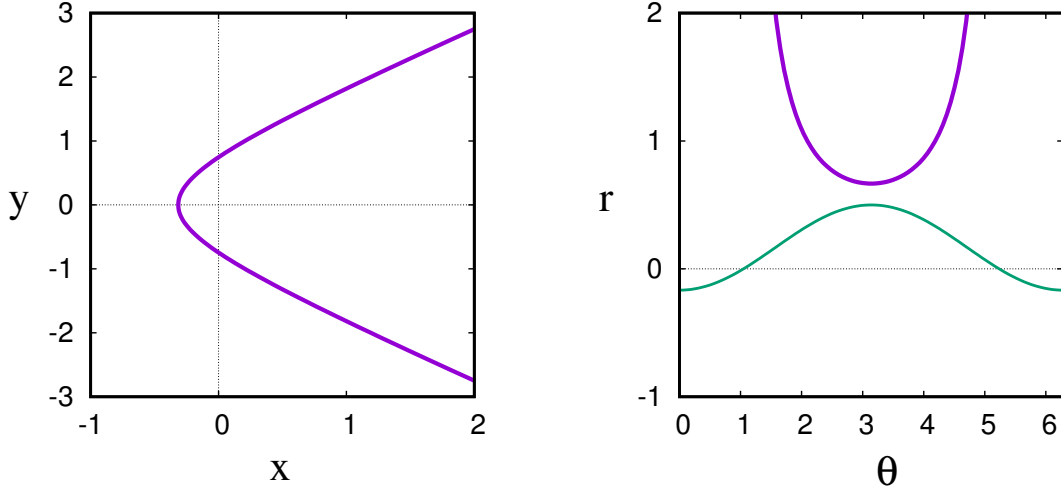


Figure ESM.1: Standard form of a hyperbola (left) as given by (ESM2.2), and the corresponding graph of r against θ from (ESM2.1), using values $d = 1$, $\gamma = 0.5$. Also shown in the right figure is $\gamma - \cos \theta$ (scaled by $\frac{1}{3}$).

suppose the range of θ on the hyperbola is $(-\alpha, \alpha)$, particularly if one uses (ESM2.3), and polar coordinates based on $X = 0$, $y = 0$. However, with the origin based as in (ESM2.1) at $x = 0$, $y = 0$, and as shown in the left diagram of figure ESM.1, it is clear that the range is actually $(\alpha, 2\pi - \alpha)$, as also seen in the right diagram. The use of the polar representation of r versus θ then makes it straightforward to assess the shape of curves such as (3.2) in the paper.

ESM.3 Growth at a corner

We refer to the geometry shown in figure ESM.2. The geometry of growth demands that

$$\begin{aligned} \theta_A + \theta_P &= \theta + \frac{\pi}{2} - \chi, \\ \gamma(\chi) &= \frac{\sin \theta_P}{\sin \theta_A}, \end{aligned} \quad (\text{ESM3.1})$$

where the dependence of γ on χ is associated with the faceted nature of plagioclase growth. We also require equilibria of surface energy at the corner,¹ and thus

$$\mu \cos \theta_A + \lambda \cos \theta_P = 1, \quad \mu = \frac{\sigma_{AL}}{\sigma_{AP}} \quad \lambda = \frac{\sigma_{PL}}{\sigma_{AP}}. \quad (\text{ESM3.2})$$

¹The reason for this is that an inequality would require an infinite supply of energy at the A-P-melt corner (for the same reason that there is a barrier to homogeneous nucleation, i.e., the surface to volume ratio becomes infinite in the corner). The same assumption is made by Jackson and Hunt (1966) in their study of lamellar eutectics.

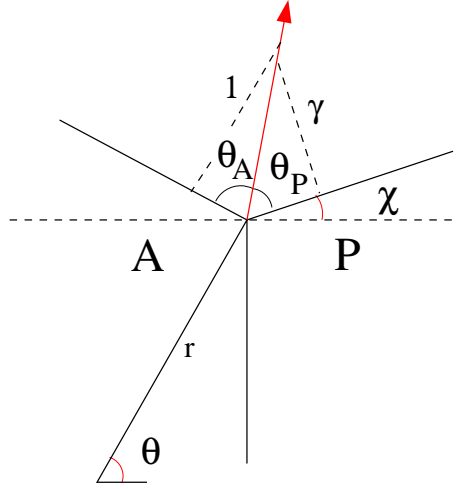


Figure ESM.2: Defining geometry at an augite-plagioclase-melt junction.

Note that we must have $\mu + \lambda > 1$. The three equations in (ESM3.1) and (ESM3.2) can be solved to determine θ_A , θ_B and χ as functions of θ .

ESM.3.1 Facetting

Before exploring the consequences of these equations, we flesh out the brief discussion of facetting in section 3.3 of the paper. Suppose we have a (two-dimensional) surface $y = s(x, t)$. We define $F = s - y$, so that the velocity of the surface \mathbf{v} satisfies

$$\frac{dF}{dt} = F_t + \mathbf{v} \cdot \nabla F = 0 \quad (\text{ESM3.3})$$

(partial derivatives with respect to t are denoted by subscripts, as in F_t), and since the upward normal is $\mathbf{n} = -\frac{\nabla F}{|\nabla F|}$, this determines the normal velocity of the interface (upwards) as

$$v_n \equiv \mathbf{v} \cdot \mathbf{n} = \frac{F_t}{|\nabla F|} = \frac{s_t}{(1 + s_x^2)^{1/2}}. \quad (\text{ESM3.4})$$

So if the interfacial growth rate is prescribed as a function of slope, $v_n = V(s_x)$, then the evolution of s is determined by solving the partial differential equation

$$s_t = V(s_x)(1 + s_x^2)^{1/2}, \quad (\text{ESM3.5})$$

where, as for t derivatives, subscripts x denote partial x derivatives.

This first order equation can be solved using Charpit's method (e.g., Carrier and Pearson 1976, chapter 12). We define

$$p = s_x, \quad Q(p) = V(p)(1 + p^2)^{1/2}; \quad (\text{ESM3.6})$$

then the solution of (ESM3.5) is obtained by solving the ordinary differential (characteristic) equations

$$\begin{aligned}\dot{x} &= -Q', \\ \dot{s} &= Q - pQ',\end{aligned}\tag{ESM3.7}$$

where Q' is the derivative of $Q(p)$, and the overdots represent time derivatives along curves in (x, t) space called characteristics, on each of which (in this example) p is constant. We parameterise the initial data $s = s_0(x)$ at $t = 0$ by specifying

$$x = x_0(\xi), \quad s = s_0(\xi), \quad p = \frac{s'_0(\xi)}{x'_0(\xi)} \quad \text{at } t = 0,\tag{ESM3.8}$$

and each characteristic curve is parameterised by ξ (and p is constant on each characteristic).

The solution is then given by

$$\begin{aligned}x &= x_0(\xi) - Q't, \\ s &= s_0(\xi) + (Q - pQ')t.\end{aligned}\tag{ESM3.9}$$

The characteristics are straight lines, and ‘shocks’ will form if they intersect. These shocks correspond to the formation of facets. It is easier to deal with the surface angle $\psi \equiv \chi$, where $p = \tan \psi$, rather than the slope p , and we will take $V = V(\psi)$. (The angle ψ was denoted as χ in the paper, to avoid confusion with the impingement angle, but no such confusion should arise here, and ψ is the common notation in intrinsic coordinates.) Thus we find

$$\begin{aligned}Q &= \frac{V}{\cos \psi}, & Q' &= R(\psi) = V' \cos \psi + V \sin \psi, \\ Q - pQ' &= S(\psi) = V \cos \psi - V' \sin \psi;\end{aligned}\tag{ESM3.10}$$

here the prime on Q' is a derivative with respect to p , but that on V' is with respect to ψ . We can then use ψ as the characteristic parameter in (ESM3.9), which then has the form

$$\begin{aligned}x &= x_0(\psi) - R(\psi)t, \\ s &= s_0(\psi) + S(\psi)t.\end{aligned}\tag{ESM3.11}$$

Suppose first that V is constant (and positive), and that the initial configuration is a rounded corner, as shown in figure ESM.3. Then $x_0(\psi)$ is monotonically decreasing, and so $R = V \sin \psi$ is positive and decreases from V at the left to 0 at the right, and the characteristics spread out in a fan, as shown in figure ESM.3. In this case, the rounded corner grows with time, and a small seed crystal would end up being completely rounded.

However, if V is not constant, then R may not be an increasing function of ψ . Calculating its derivative, we find

$$R' = (V'' + V) \cos \psi,\tag{ESM3.12}$$

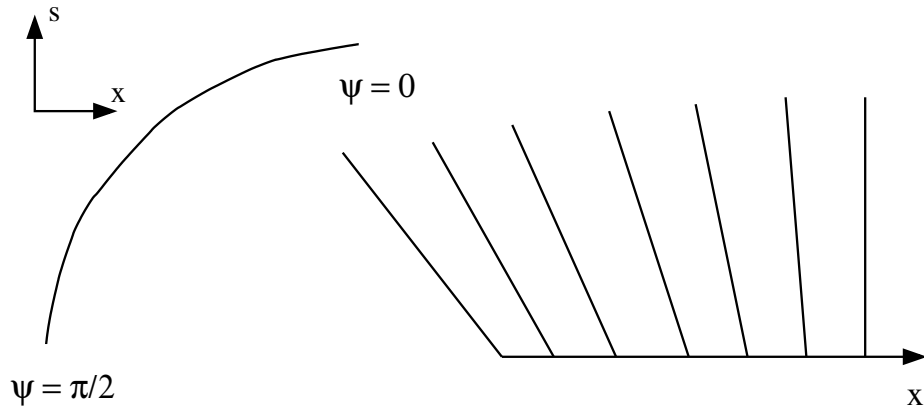


Figure ESM.3: An initially round corner remains round if V is constant.

and thus if V increases between $\psi = 0$ and $\psi = \frac{\pi}{2}$, R may have an interior maximum at ψ_M , say. An example of such a pair is shown in figure ESM.4. In this case, the characteristic from $x = x_M$ where $\psi = \psi_M$ is the most steeply inclined to the left, and so it will catch up with all those to the left of x_M . A shock will form, representing the formation of a corner, where eventually the surface angle jumps from $\frac{\pi}{2}$ to ψ_M , as indicated in figure ESM.5. To the right of x_M , the characteristics spread out as a fan, and a curved upper face is propagated. However, if the maximum of R is at $\psi = 0$, which will be the case if V increases sufficiently rapidly near $\psi = 0$, then the most steeply inclined characteristics are those at the far right, there is no fan, and the eventual shape is a right-angled facet.

For the mathematician, it is perhaps easier to see what happens by taking the x derivative of (ESM3.5). This gives the hyperbolic equation

$$p_t - Q'(p)p_x = 0, \tag{ESM3.13}$$

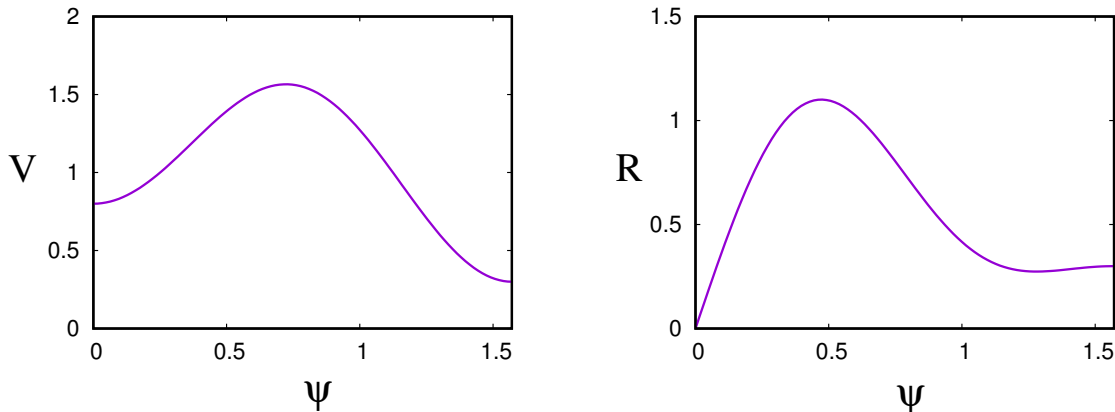


Figure ESM.4: The functions $V(\psi)$ (left) and $R(\psi)$ (right) given by $V = 0.8 \cos^2 \psi + 0.3 \sin^2 \psi + \sin^2 2\psi$; R is defined in (ESM3.10).

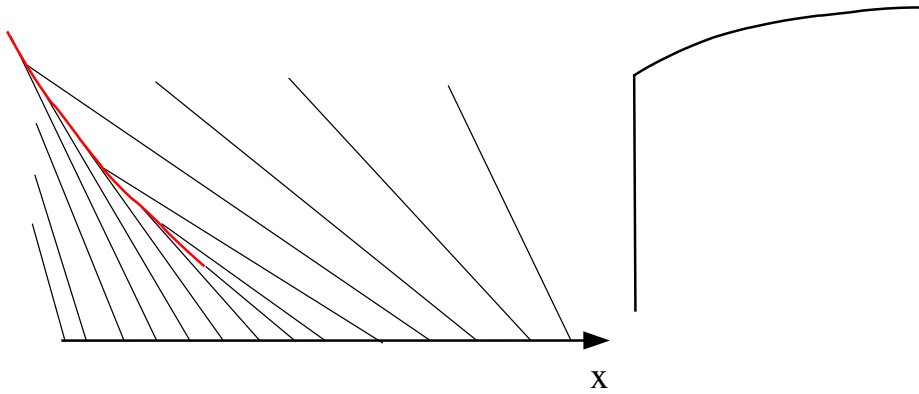


Figure ESM.5: Shock and facet formation when $R(\psi)$ has an interior maximum.

or better, in terms of ψ ,

$$\psi_t - R(\psi)\psi_x = 0. \quad (\text{ESM3.14})$$

Shocks form as described above if $R' < 0$, and at these there is a jump in ψ and thus slope.

ESM.3.2 The rôle of curvature

The Gibbs-Thomson effect depresses the liquidus temperature due to curvature of the interface. Suppose the ambient liquidus temperature is T_L , and the actual local temperature is T_0 , so that the local undercooling is $\Delta T = T_L - T_0$ at a planar interface. We might for example specify the growth rate as $V(\psi) = \Gamma(\psi)\Delta T$. If the interface is curved, the Gibbs-Thomson effect implies that the (local equilibrium) interfacial undercooling is

$$\Delta T_i = \Delta T - \frac{2\sigma T_L \kappa}{\rho_s L}, \quad (\text{ESM3.15})$$

where κ is the mean curvature, measured from the solid side, σ is surface energy, ρ_s is solid density, and L is latent heat. This suggests that for a curved interface, we take the growth rate to be $V(1 - \delta\kappa)$, where, if the model is written dimensionlessly in terms of a grain length scale d_g , the (then dimensionless) parameter δ would be

$$\delta = \frac{2\sigma T_L}{\rho_s L d_g \Delta T}, \quad (\text{ESM3.16})$$

and the modification of (ESM3.5) would be

$$s_t = V(s_x)(1 + s_x^2)^{1/2} \left[1 + \frac{\delta s_{xx}}{(1 + s_x^2)^{3/2}} \right], \quad (\text{ESM3.17})$$

using the definition of curvature for $s(x, t)$.

This curvature term has a diffusive effect. We can write (ESM3.17) in the form

$$s_t = Q(p) + \delta V(p)[\tan^{-1} p]_x, \quad (\text{ESM3.18})$$

and differentiating,

$$p_t - Q'(p)p_x = \delta[V(p)\{\tan^{-1} p\}_x]_x, \quad (\text{ESM3.19})$$

which also shows its diffusive nature. This term can thus provide a shock structure which smoothes jumps in slope over a (dimensionless) distance $\sim \delta$. In detail, near a shock $x_s(t)$ moving at speed $-c$ (c positive so leftward moving as in figure ESM.5), we put $x = x_s + \delta X$, and then approximately

$$cp_X - [Q(p)]_X = [V(p)\{\tan^{-1} p\}_X]_X, \quad (\text{ESM3.20})$$

with first integral

$$K + cp - Q(p) = V(p)\{\tan^{-1} p\}_X, \quad (\text{ESM3.21})$$

and the solution of this provides the shock structure joining values p_{\pm} in $x \gtrless x_s$.

ESM.3.3 Beaking

Having elucidated how faceting occurs in a growth model, we now return to the consideration of growth at an augite-plagioclase-melt corner, as described by the solution of the equations in (ESM3.1) and (ESM3.2). First we seek to understand whether the problem is well-posed. We can consider a situation where augite and plagioclase crystals grow upwards in a finite (dimensionless) domain $0 < x < 1$, say, with symmetric or periodic boundary conditions, so that $s_x = 0$ at $x = 0, 1$. We denote the location of the A-P-melt junction as $x = \alpha(t)$. It follows from figure ESM.2 that α is determined by

$$\dot{\alpha} = \frac{\sin(\theta_A - \theta)}{\sin \theta_A}. \quad (\text{ESM3.22})$$

We need to solve (ESM3.17) separately in $x \gtrless \alpha$, with conditions of continuity of s at $x = \alpha$, together with (ESM3.1) and (ESM3.2). Suppose we take $s = s_c$ at $x = \alpha$. Then we have enough boundary conditions to solve for s , and thus determine s_x at $\alpha \pm$, which determines θ and χ in terms of s_c . The three equations in (ESM3.1) and (ESM3.2) then determine θ_A and θ_P , with the extra equation providing the value of s_c .

Now we consider what happens to this well-posed problem if δ is small. As already described, the singular approximation $\delta \rightarrow 0$ makes the growth problem hyperbolic. At the plagioclase corner, the shock structure is replaced by an actual shock, but there is a genuine discontinuity in slope at the A-P-melt junction. The loss of the diffusive term implies the loss of ability to satisfy all three conditions in (ESM3.1) and (ESM3.2), and as we have supposed all along, the one that is lost is the surface energy balance (ESM3.2). On the long plagioclase face, we then have $\chi = \frac{\pi}{2}$, θ is given from the radial augite growth, and (ESM3.1) determines θ_A and θ_P . The actual satisfaction of (ESM3.2) then requires a boundary layer of thickness $O(\delta)$, in which χ changes from its actual value at the junction to $\frac{\pi}{2}$ on the vertical plagioclase face.

The issue that then faces us is what happens when the boundary layer at the A-P-melt junction runs into the shock structure at the plagioclase corner. The eventual

outcome is that a new A-P-melt boundary layer propagates along the short face, having destroyed the corner shock structure, and our conjecture is that this can not happen instantly, but requires a finite time while the slow evolution of θ allows the adjustment to take place. However, a detailed demonstration of the validity of this conjecture is somewhat challenging.

ESM.4 Derivation of (4.1)

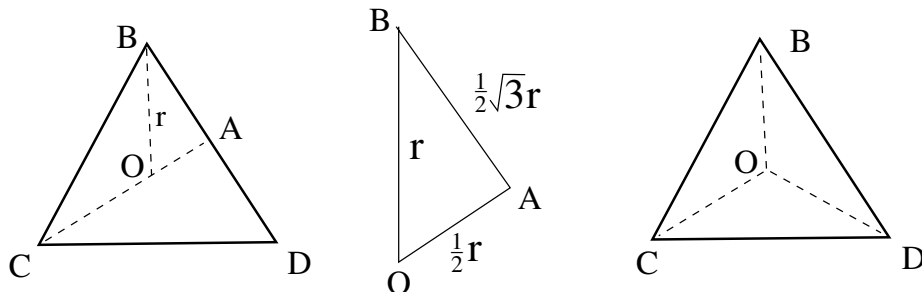


Figure ESM.6: The geometry of pore close-off.

For simplicity we will suppose that there is no change of volume on solidification. On the left we see an equilateral triangle BCD whose circumcircle has radius OB of length r . As shown in the blown-up triangle OAB, the lengths of AB and OA are $\sqrt{3}r$ and $\frac{1}{2}r$ respectively, since the angle $\angle OBA = 30^\circ$, and $\sin 30^\circ = \frac{1}{2}$, $\cos 30^\circ = \frac{1}{2}\sqrt{3}$. Therefore the length of a side such as BD is $\sqrt{3}r$, while an altitude such as COA is of length $\frac{3}{2}r$; so the area of BCD is $\frac{3\sqrt{3}}{4}r^2$. If μ_L is the chemical potential (J mole $^{-1}$), then μ_L/V_M is the chemical potential in J m $^{-3}$, where V_M is the molar volume (m 3 mole $^{-1}$). The free energy of the liquid in BCD per unit length transverse to the page is thus

$$G_L = \frac{3\sqrt{3}r^2\mu_L}{4V_M} + 3\sigma_{PL}\sqrt{3}r, \quad (\text{ESM4.1})$$

where the second term is the surface energy of the three solid-liquid interfaces BC, CD and DB.

In the final solidified state, the volumetric free energy is similar (replace μ_L by μ_S), but the solid-solid surface energy σ_{PP} replaces σ_{PL} , and the new surface area per unit length out of the page is the sum of the lengths of OC, OB and OD, each of which is of length r . Hence we have

$$G_S = \frac{3\sqrt{3}r^2\mu_S}{4V_M} + 3\sigma_{PP}r, \quad (\text{ESM4.2})$$

and thus the free energy per unit length out-of-page of the liquid prism in figure 8 of the paper relative to the solid state is

$$\Delta G = G_L - G_S = \frac{3\sqrt{3}r^2\Delta\mu}{4V_M} + 3\left(\sigma_{PL}\sqrt{3} - \sigma_{PP}\right)r, \quad (\text{ESM4.3})$$

where $\Delta\mu = \mu_L - \mu_S$.

ESM.5 Equilibrium dihedral angle

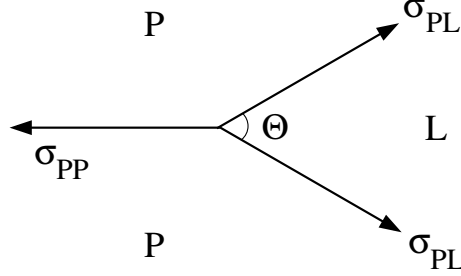


Figure ESM.7: The equilibrium dihedral angle

The equilibrium angle between two plagioclase grains and liquid (mentioned following equation (4.1)) satisfies

$$\sigma_{PP} = 2\sigma_{PL} \cos \frac{1}{2}\Theta. \quad (\text{ESM5.1})$$

The reason for this is that we can interpret the minimisation of surface energy in terms of an apparent force (the surface tension) acting along the interfaces. Thus in figure ESM.7, the interfacial forces per unit length (in the page) are σ_{PP} and σ_{PL} , and resolving these in the horizontal with a dihedral angle Θ leads to (ESM5.1).

ESM.6 Derivation of (4.3) from (4.2)

For the situation shown in figure ESM.8 (figure 10 of the paper, slightly modified), the surface energy increment is defined by

$$E = \sigma_{PP}RS + 2\sigma_{AP}PQ + \sigma_{AL}PV + 2\sigma_{PL}PS. \quad (\text{ESM6.1})$$

In order to derive (4.3) in the paper, we need to show that (the lengths of)

$$\begin{aligned} RS &= \frac{\int_0^\tau \gamma(s) ds}{\sin \alpha}, & PQ &= \int_\alpha^\theta [R'(\theta')^2 + R(\theta')^2]^{1/2} d\theta', \\ PV &= (\pi - 2\theta)R(\theta), & PS &= \frac{R(\theta) \cos \theta}{\sin \alpha}. \end{aligned} \quad (\text{ESM6.2})$$

We consider these four line segments in turn.

The curve UTQ is the circular arc $r = r_0$, where the polar coordinates (r, θ) are as shown in the figure. The right hand plagioclase-liquid interface RQ is the straight line $r \cos(\theta - \alpha) = r_0$. At later values τ of the time-like variable defined in (2.1) of

References

- Carrier, G. F. and C. E. Pearson 1976 Partial differential equations. Academic Press, New York.
- Jackson, K. A. and J. D. Hunt 1966 Lamellar and rod eutectic growth. Trans. Metall. Soc. AIME **236** (8), 1,129-1,141.